# Expanded View Figures

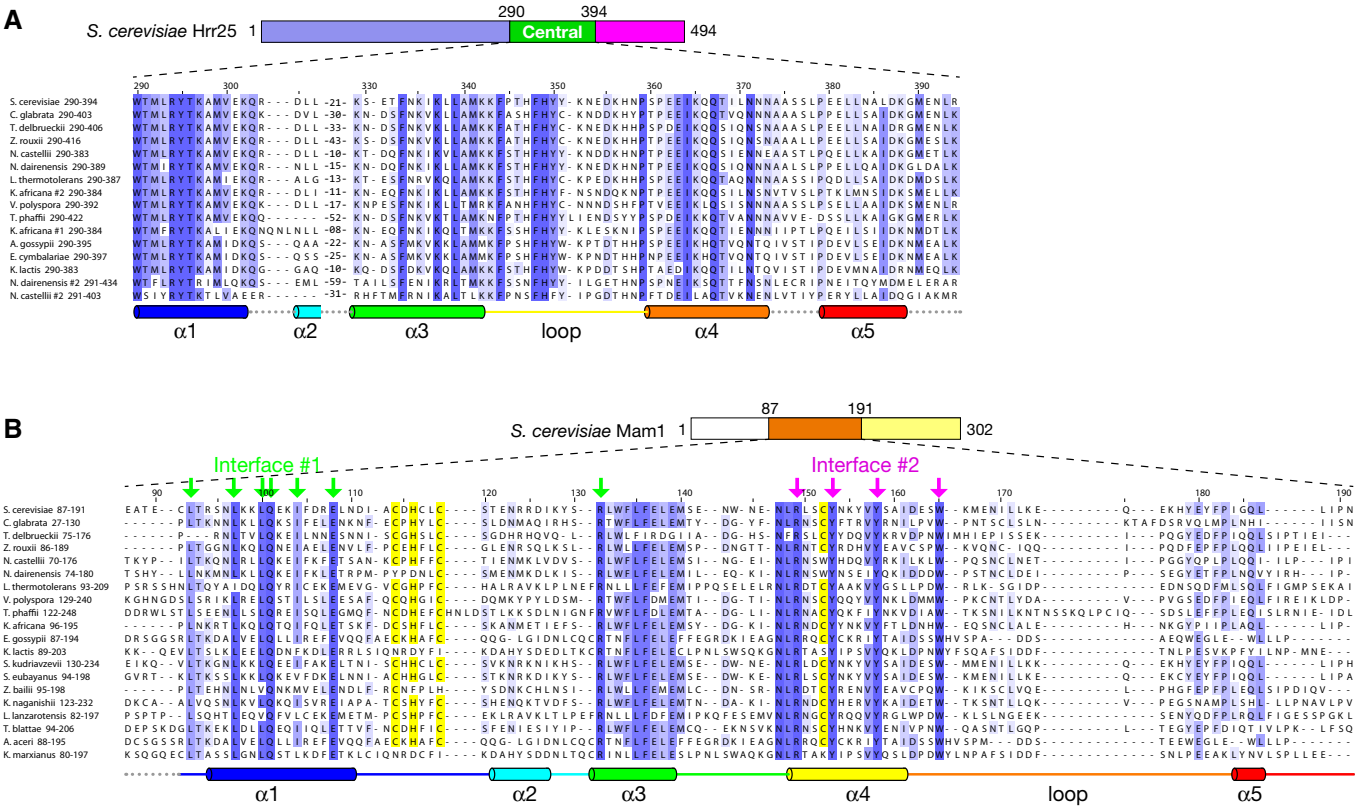


**Figure EV1. Sequence alignments of the Hrr25 central domain and the Hrr25-binding region of Mam1.**

A Sequence alignment of the Hrr25 central domain from the Saccharomycotina fungi (green branches in Fig 1B).

B Sequence alignment of the Mam1–Hrr25-binding region from the same set of Saccharomycotina fungi. Shown in yellow are conserved zinc-coordinating cysteine and histidine residues (see Fig 4). Green and magenta arrows mark residues involved in Hrr25 interfaces #1 and #2, respectively (see Fig 5).

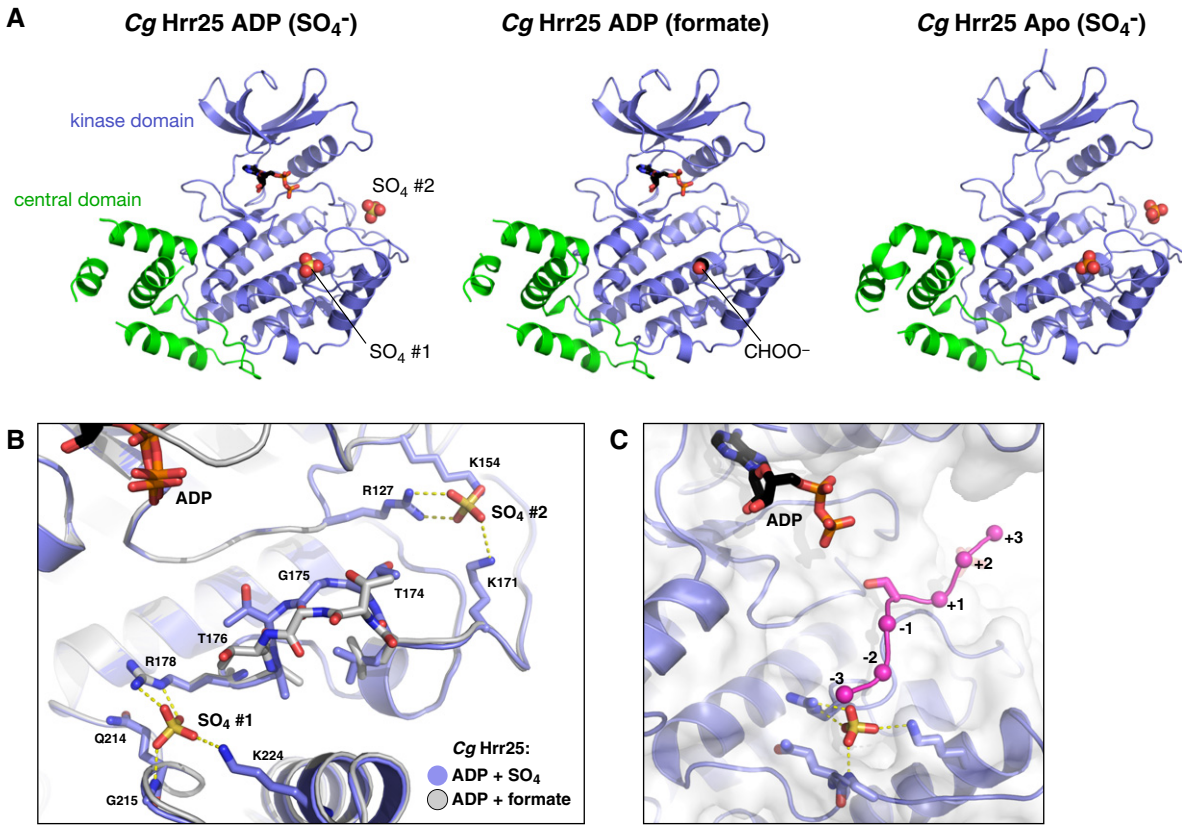


**Figure EV2. $PO_4^-$ binding sites in Hrr25.**

A Aligned structures of *Candida glabrata* $Hrr25^{1–403}$ crystallized without nucleotide (Apo, left), or in the presence of ADP in crystallization buffer with formate (center) or sulfate ($SO_4^-$, right). $PO_4^-/SO_4^-$ ions bound to sites 1 and 2 are shown as spheres. In the ADP (formate) structure, there is no ion bound to site 2, but a formate ion ($CHOO^-$) is observed at site 1.

B Close-up view of $PO_4^-$ binding sites S1 and S2 in *C. glabrata* Hrr25 (blue), overlaid with the formate-bound structure (white).

C View of the *C. glabrata* Hrr25 active site and $SO_4^-$ at S1, with modeled substrate peptide from a Cdk2:cyclin A:peptide complex (PDB ID 1GY3) (Cook *et al*, 2002).

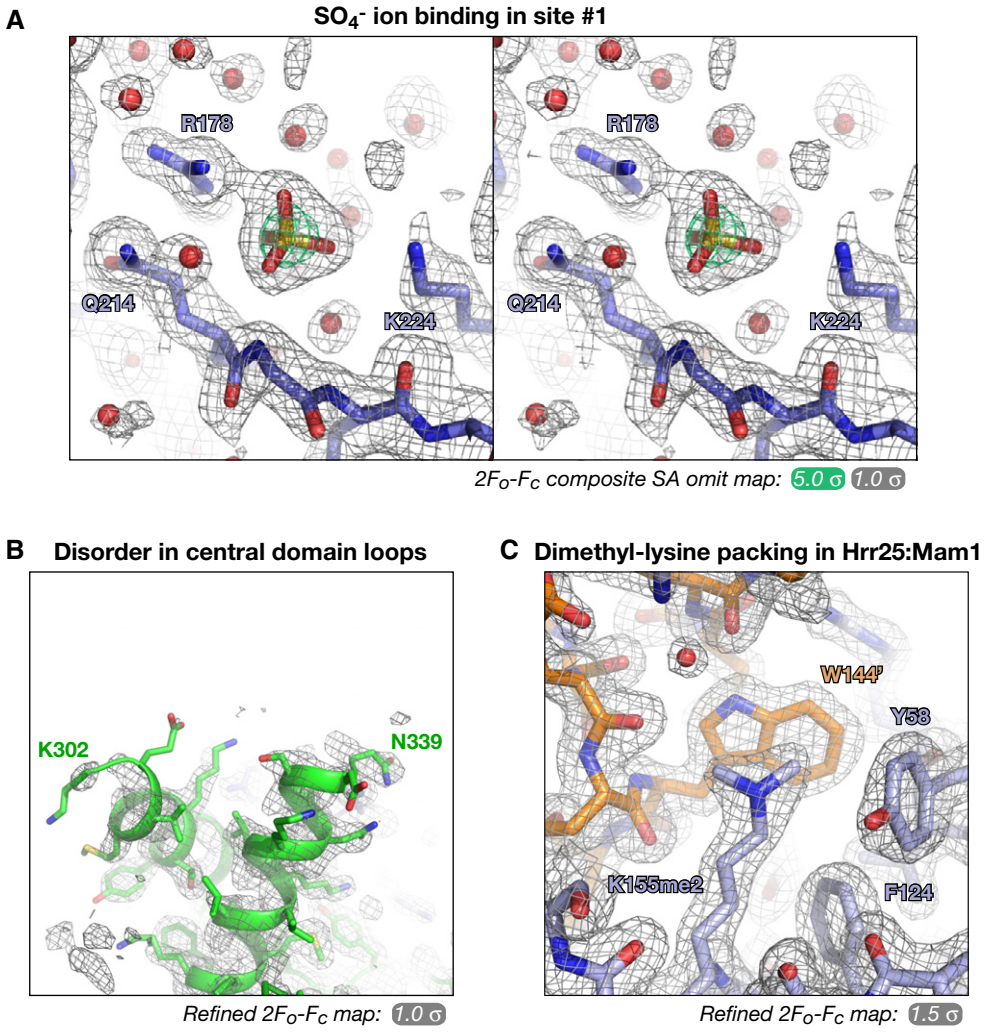


**Figure EV3. Representative electron density maps.**

A Stereo view of a $2F_o–F_c$ simulated-annealing composite all-omit map from the *Candida glabrata* Hrr25$^{1–403}$·ADP complex (2.0 Å resolution), showing the sulfate ion bound to site #1.

B Refined $2F_o–F_c$ electron density for the α1–α3 segment (α2 is disordered in this structure) Hrr25 central domain in the *C. glabrata* Hrr25$^{1–403}$·ADP complex (2.0 Å resolution).

C Example crystal packing interaction mediated by dimethylated surface lysine residues in the structures of *S. cerevisiae* Hrr25$^{1–394}$ K38R:Mam1$^{87–191}$. Here, dimethylated Hrr25 Lys155 (foreground; blue) forms a hydrophobic packing interaction with a symmetry-related Mam1 Trp144 (background; orange). Refined $2F_o–F_c$ electron density is shown at 1.5 σ.

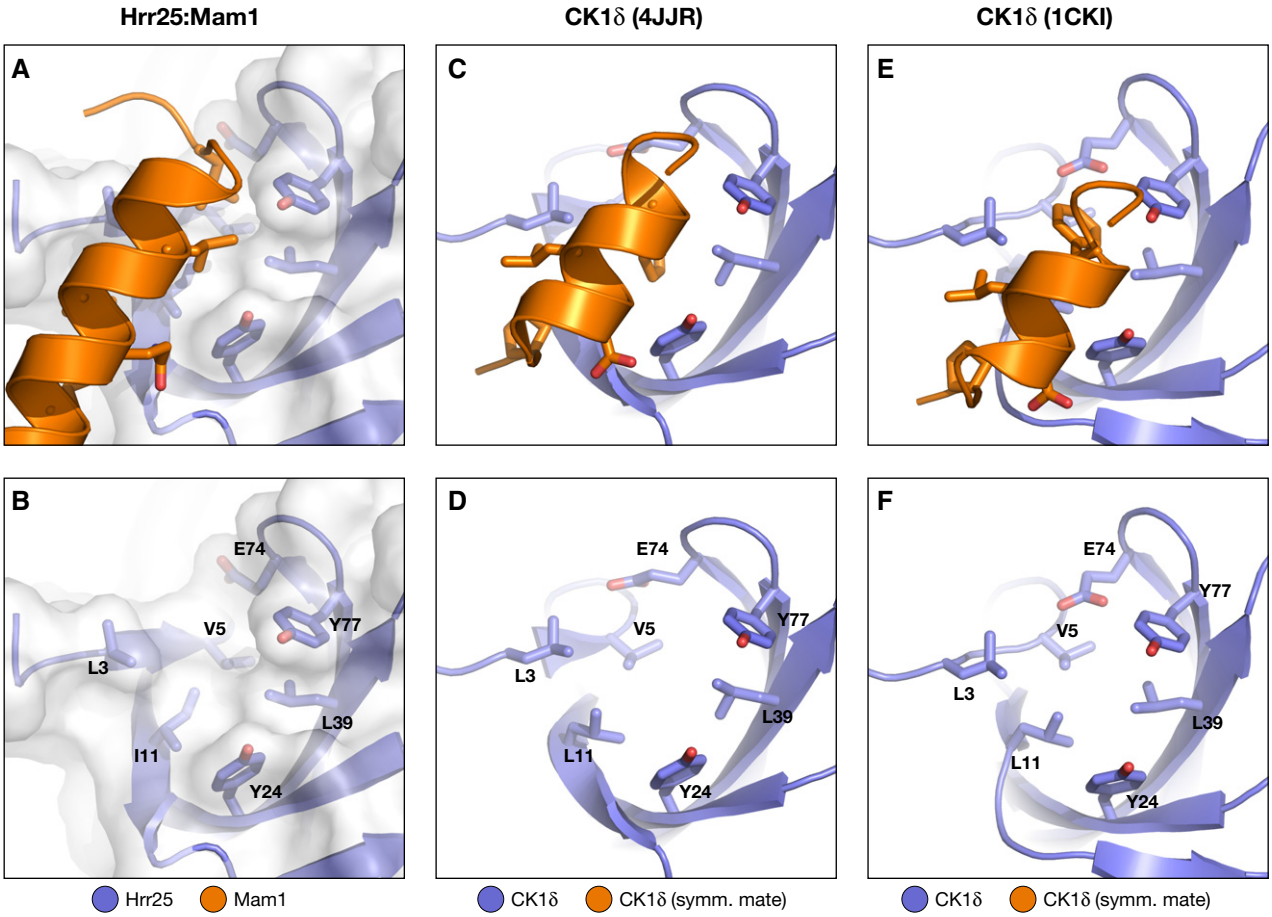


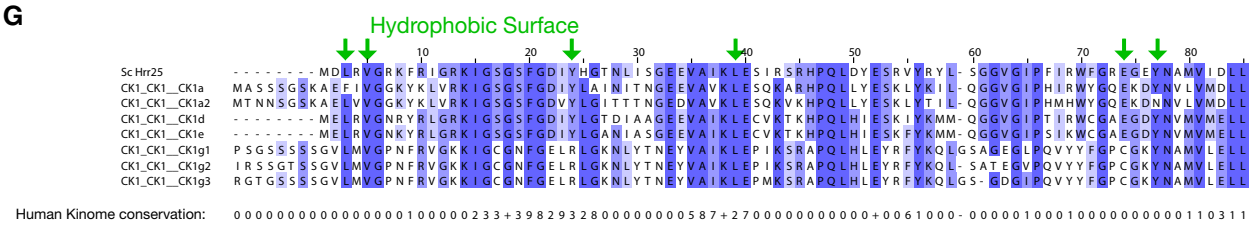


**Figure EV4. Conservation of N-lobe hydrophobic surface in CK1-family kinases.**

A–F Views of the kinase domain N-lobes of Hrr25 (A, B), human CK1δ in PDB 4JJR (C, D) (Zeringo *et al*, 2013), and human CK1δ in PDB 1CKI (E, F) (Longenecker *et al*, 1996). Upper panels show kinase domain (blue) with conserved hydrophobic surface residues in stick view and bound α-helix from Mam1 (A) or a symmetry-related copy of CK1δ (C, E) in orange. Lower panels are missing bound partner for clarity, with conserved hydrophobic surface residues labeled.

G Sequence alignment of the Hrr25 N-lobe with all human CK1-family kinases. At bottom is shown the conservation score (1–10, "+" indicates a score of 10) calculated by Jalview from an alignment of the entire human kinome (downloaded from http://kinase.com) plus Hrr25. Hydrophobic surface residues are shown with green arrows; most of these residues are highly conserved within CK1-family kinases but poorly conserved in kinases as a whole.

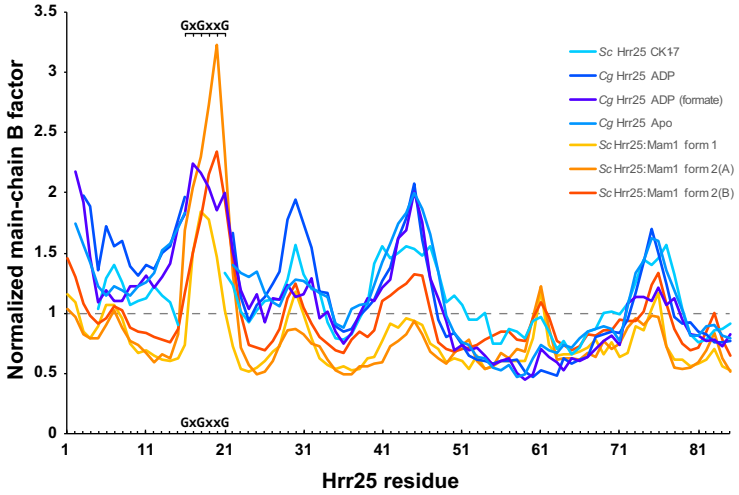


**Figure EV5. N-lobe B-factors for Hrr25 and Hrr25:Mam1 structures.**
Residue-by-residue plot of main-chain B-factors from four structures of Hrr25 and three crystallographically unique views of Hrr25:Mam1. Values are normalized as in Fig 6D, with the average B-factor for the entire Hrr25 chain adjusted to 1.0. Values calculated with BAVERAGE (Winn *et al*, 2011). GxGxxG indicates the glycine-rich loop (residues 16–21 in both *Saccharomyces cerevisiae* and *Candida glabrata* Hrr25) that drapes over a bound nucleotide. This motif is well ordered in all three views of Hrr25:Mam1, but only one of the four structures of Hrr25. Because the GxGxxG motif was disordered in three of four Hrr25-alone structures and was therefore not included in the analysis in Fig 6D, that analysis likely underestimates the stabilizing effect of Mam1 on Hrr25 structure.

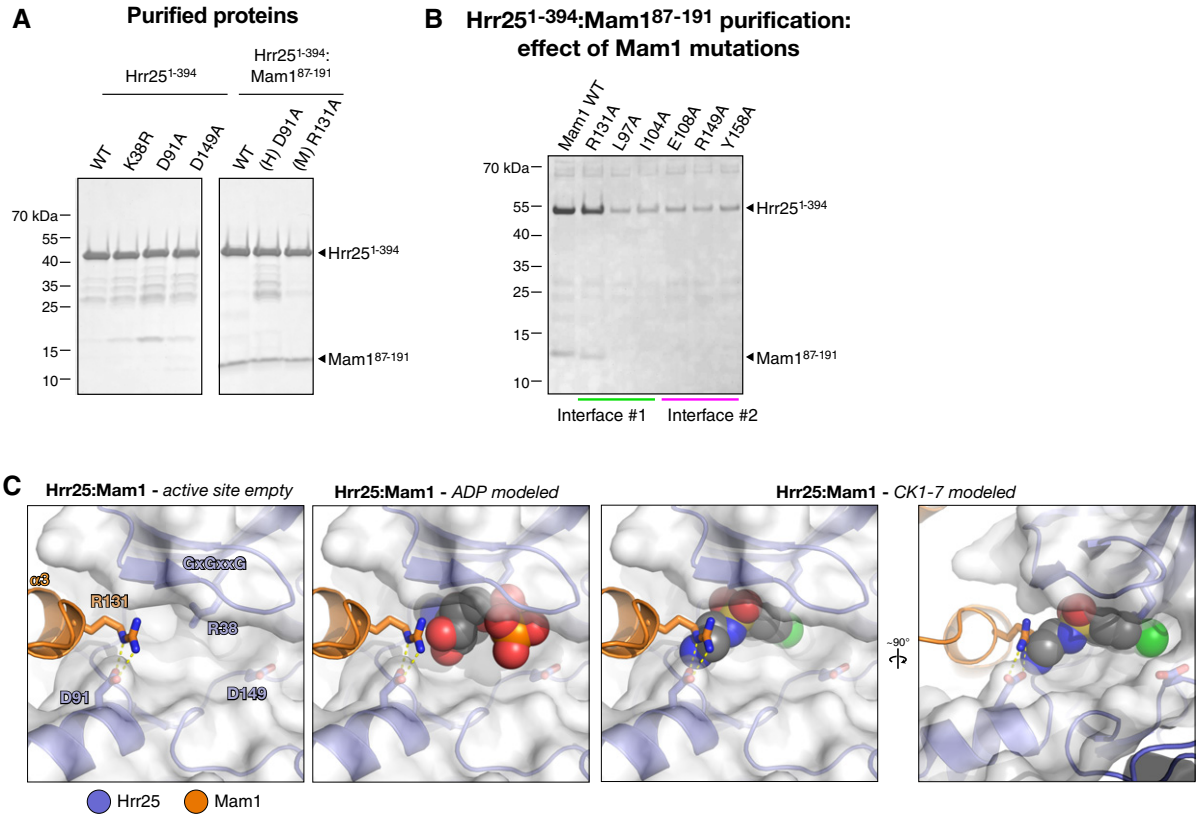


**Figure EV6. Purification of Hrr25 and Hrr25:Mam1 for ATPase assays and modeling of Mam1 Arg131 interaction with nucleotide and CK1-7.**

A SDS–PAGE analysis of purified *Saccharomyces cerevisiae* Hrr25$^{1–394}$ and Hrr25$^{1–394}$:Mam1$^{87–191}$ complexes used for ATPase assays.

B $Ni^{2+}$ affinity pull-down of co-expressed $His_6$-Hrr25$^{1–394}$ K38R:Mam1$^{87–191}$ complexes with mutations to Mam1 in interfaces #1 or #2. Except for R131A, all mutations result in a loss of co-purification of Mam1, indicating a loss of binding, and a significant reduction in the level of soluble Hrr25$^{1–394}$ K38R.

C Close-up views of the Hrr25 active site in the structure of *S. cerevisiae* Hrr25$^{1–394}$:Mam1$^{87–191}$. Mam1 R131 extends toward the ATP-binding pocket, and while it would not clash with a bound nucleotide (center panel), it would clash with the aminoethyl group of bound CK1-7 (right panels).